Biol. Cybern. 64, 41–49 (1990)

Biological Cybernetics

Applicability of quadratic and threshold models to motion discrimination in the rabbit retina

Norberto M. Grzywacz [1,2], F. R. Amthor [3], and L. A. Mistler [1]

[1] Center for Biological Information Processing, Department of Brain and Cognitive Sciences, Massachusetts Institute of Technology, E25-201, Cambridge, MA 02139, USA
[2] The Smith-Kettlewell Eye Research Institute, 2232 Webster Street, San Francisco, CA 94115, USA
[3] Department of Psychology, University of Alabama at Birmingham, Birmingham, AL 35294, USA

Received March 7, 1990/Accepted in revised form May 28, 1990

Abstract. Computational and behavioral studies suggest that visual motion discrimination is based on quadratic nonlinearities. This raises the question of whether the behavior of motion sensitive neurons early in the visual system is actually quadratic. Theoretical studies show that mechanisms proposed for retinal directional selectivity do not behave quadratically at high stimulus contrast. However, for low contrast stimuli, models for these mechanisms may be grouped into three categories: purely quadratic, quadratic accompanied by a rectification, and models mediated by a high level threshold. We discriminated between these alternatives by analyzing the extracellular responses of ON-OFF directionally selective ganglion cells of the rabbit retina to drifting periodic gratings. The data show that purely-quadratic or high-threshold systems do not account for the behavior of these cells. However, their behavior is consistent with a rectified-quadratic model.

Introduction

Computational models of visual motion discrimination have been proposed for the behavior of insects (Hassenstein and Reichardt 1956) and humans (van Santen and Sperling 1984; Adelson and Bergen 1985). In these models, a few spatially separated linear filters preprocess the image and interact through quadratic nonlinearities (Poggio and Reichardt 1973). These nonlinearities are multiplicative-like mechanisms, which have some optimal properties for motion information processing (Poggio and Reichardt 1973).

Although evidence suggests that organisms behave as quadratic detectors (Hassenstein and Reichardt 1956; van Santen and Sperling 1984; Adelson and Bergen 1985), it is unclear whether motion sensitive neurons do so. An important class of motion sensitive neurons consists of the directionally selective cells (Hubel and Wiesel 1959; Maturana et al. 1960; Barlow and Levick 1965; Schiller et al. 1976; Hausen 1981). These are neurons that respond strongly to stimuli moving in a particular (preferred) direction and weakly to stimuli moving in the opposite (null) direction. It is unlikely that directionally selective cells behave quadratically at high stimulus contrast, due to nonlinearities evoked under those conditions (Grzywacz and Koch 1987). However, at low contrast, the behavior of some proposed neural mechanisms for directional selectivity may be approximately quadratic (Thorson 1966; Torre and Poggio 1978). In this paper, we test whether ON-OFF directionally selective ganglion cells in the rabbit retina behave as quadratic detectors of low contrast motion stimuli.

To test for quadratic behavior, we first study theoretically its predictions for drifting spatially periodic gratings. Then, still theoretically, these predictions are compared to two other plausible models for directional selectivity. Finally, we test whether these predictions hold for the ganglion cells' extracellular responses.

Our theoretical models are described in terms of computational elements, rather than by explicit neural mechanisms. However, the Section "Theory" discusses the neural interpretations of these models. Furthermore, these are high-level models that may lump several neural processes, and thus may be closer to animal behavior. This level of modeling fits the scope of this paper, which is the overall behavior of directionally selective cells. This scope justifies the use of extracellular recordings, which unfortunately cannot tell in what retinal cells the interactions that mediate directional selectivity occur. Nevertheless, such recordings take into account "contaminations" by neural processes other than the ones involved in directional selectivity.

In the next section, we describe the three theoretical models and their predictions. The second portion of this paper reports on experiments that tested these predictions and discusses the experimental results.

Theory

This section is divided in three parts in the following way. The first, which is called "Neural Basis", describes

the physiological and anatomical rationales for the three models that we test. Then, the subsection "Models" presents the mathematical formalization of the models. The third part, "Predictions," explains the properties we use to distinguish between the models.

1 Neural basis

A spatially asymmetric inhibition underlies some of the important properties of retinal directional selectivity (Barlow and Levick 1965). To produce directionality, the mechanism for this inhibition must work through a nonlinearity (Poggio and Reichardt 1973). In fact, a linear inhibition could alter the time course of the response, but not its total time integral (for example, the total number of spikes).

A nonlinear inhibitory mechanism that has been proposed for directional selectivity is synaptic shunting inhibition (Thorson 1966; Torre and Poggio 1978). According to this proposal, such synapses do not lead to the hyperpolarization of the postsynaptic cell. Rather, they inhibit the postsynaptic dendritic tree via a reduction of its membrane resistance. Thus, since changes of membrane resistance do not propagate throughout the dendritic tree like membrane voltage, the dendritic tree is affected in a relatively local way. This locality can be an asset for models of retinal directional selectivity. The dendritic locality could account for the locality of the computation of retinal directional selectivity as demonstrated by Barlow and Levick (1965). They found that motions spanning distances smaller than the receptive field size and delivered almost anywhere in the receptive field elicit directionally selective responses (Barlow and Levick 1965). In the rabbit, the directionally selective ganglion cells morphology is well suited for shunting inhibition locality (Amthor et al. 1984; Amthor et al. 1989). The "starburst" amacrine cells, which contribute to directional selectivity (Masland et al. 1984), may also be suited (Miller and Bloomfield 1983). Evidence for shunting-inhibition-based directional selectivity was found in the turtle (Marchiafava 1979), frog (Watanabe and Murakami 1984), and more recently, in the rabbit (Amthor and Grzywacz 1990).

An alternative nonlinear inhibitory mechanism that has been proposed for retinal directional selectivity is based on threshold (Grzywacz and Koch 1987). In its extreme form, this mechanism uses a hyperpolarizing synapse, whose synaptic potential subtracts from the effects of a depolarizing synapse. The result of this subtraction is then passed through a threshold operation. This inhibition could be local if, for example, the threshold is due to the synaptic release from an amacrine cell's dendrite (Grzywacz and Koch 1987). (Directional selectivity based on threshold would probably be presynaptic to the ganglion cells; Grzywacz and Koch 1987.) Evidence for a threshold-based directional selectivity was found in ON and OFF ganglion cells of the frog (Watanabe and Murakami 1984).

The behavior of shunting-inhibition-based directional selectivity is approximately quadratic at low contrast stimuli (Thorson 1966; Torre and Poggio 1978). So is a directional selectivity based on a smooth threshold (Grzywacz and Koch 1987). Such threshold may be, for example, a synaptic threshold that is not high when compared to the resting presynaptic potential (like in photoreceptor synapses; Dowling 1979). These low-contrast quadratic behaviors are analogous to the approximation of a smooth function by the linear and quadratic terms of its Taylor expansion when the function's argument is small.

However, these considerations do not prove that directional selectivity is quadratic at low contrast stimuli. Two plausible alternative low contrast behaviors must be considered. In the first, rectifications not associated with the directionally selective mechanism may either precede or follow the quadratic inhibition. In fact, rectifications might be fundamental in retinal information processing (Victor and Shapley 1979). They are associated with the ON and OFF inputs (Kuffler 1953; Famiglietti et al. 1977) to amacrine and ganglion cells, and with the ganglion cells' spiking mechanism. The second alternative is a directional selectivity based on a high threshold (Grzywacz and Koch 1987). Such threshold might operate, for example, at the level of transmitter release from amacrine cells. According to this mechanism, release would only occur if presynaptic voltage became sufficiently high. A quadratic behavior would not approximate this mechanism well. To understand the failure of such approximation, just consider using a Taylor expansion to approximate a function whose only significant non-zero values occur for large positive arguments. If the expansion is around zero, then one would need many terms (higher than quadratic) of the Taylor series to get a good approximation.

In summary, for low contrast stimuli, the neural mechanisms proposed for directional selectivity may be approximated by three models based on the following nonlinearities: *(1)* purely quadratic; *(2)* rectified quadratic; *(3)* high threshold. These three models are illustrated in Fig. 1.

2 Models

This section presents the three models of Fig. 1 mathematically; they appear elsewhere in more detail (Grzywacz and Koch 1987). An aspect that is common to the three models is the linear preprocessing of the image. Then, a rectification appears in the rectified-quadratic model (Fig. 1). Finally, the section introduces the two forms of nonlinearities that generate directional selectivity: quadratic and high-threshold mechanisms. Low-threshold mechanisms are not considered, because they can be approximated by quadratic nonlinearities under low contrast stimuli. Also, we do not explicitly consider the rectified versions of the high-threshold model, as the experiments described in this paper do not distinguish between linear versus rectified versions of the high-threshold model.

We assume that the only nonlinearities involved are the mechanisms that generate directional selectivity and rectifications. (This assumption is justified, because in

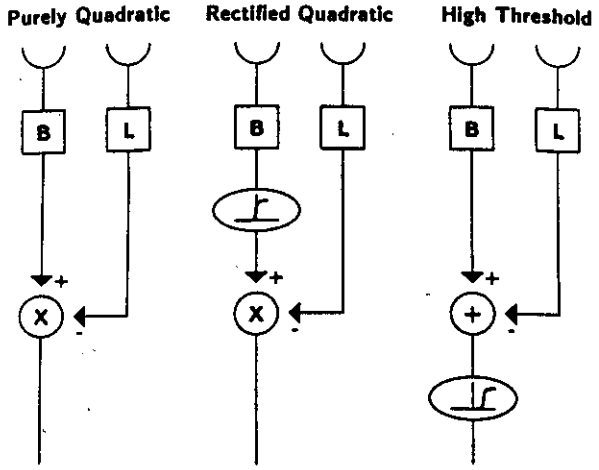

Fig. 1. The three models distinguished in this paper. Each model has two spatially-separated linear preprocessing filters. These filters have different temporal characteristics (B and L refer to the filters conceivably having band-pass and low-pass characteristics respectively), and possibly, different output polarity. The interaction between the filters is either quadratic (represented by " × ") or linear followed by a threshold operation. In the rectified-quadratic model, the output of the "B" (excitatory) filter is rectified. Both the rectification and the threshold operations appear in the figure as sigmoidal input-output relationships. The difference between these operations is that in the high-threshold model, but not in the rectified-quadratic model, the curve's rising phase is far from zero

this paper we deal with low contrast stimuli.) Now, consider a one-dimensional luminance pattern moving at constant velocity, $I(x, t) = I(x - vt)$. Before any nonlinearity intervenes, this pattern is preprocessed linearly:

$$z_k(t) = \int_{-\infty}^{\infty} \int_{-\infty}^{\infty} dx'\, dt' S_k(x', t') I(x', t - t') \quad k = e, i, \tag{1}$$

where S_e and S_i are the excitatory and inhibitory spatial-temporal filters respectively, and z_k are their outputs. (The assumption of two-filter preprocessing is only for the sake of discussion simplicity; in general any number of filters may be assumed.)

In this work, the inputs that we present to the directionally selective system are periodic, and thus have a Fourier series decomposition. The output of the linear filters (1) is

$$\begin{aligned} z_k(t) &= L_{0k} + \gamma \sum_{j=1}^{\infty} L_{jk} \cos(j\omega t - \theta_{S_k} - \phi_j), \\ L_{0k} &= I_0 \bar{S}_k(0, 0); \qquad L_{jk} = I_j \left| \bar{S}_k\left(\frac{j}{\lambda}, j\omega\right) \right|; \\ \bar{S}_k\left(\frac{j}{\lambda}, j\omega\right) &= \left| \bar{S}_k\left(\frac{j}{\lambda}, j\omega\right) \right| e^{i\theta_{S_k}(j/\lambda, j\omega)}, \end{aligned} \tag{2}$$

where I_j are the Fourier coefficients of the input (light intensity), γ is a parameter proportional to the stimulus contrast, λ is spatial frequency, ω is the angular velocity of the pattern, ϕ_j is the phase of the jth Fourier component of the input, and the tilde stands for Fourier transform in both space and time.

To introduce the rectifications, we assume that the excitatory pathway is rectified. Also, it is assumed that these rectifications appear in the visual pathway before the interactions that generate directional selectivity. (This assumption does not modify the validity of our conclusions.) In this case, the ON-OFF inputs to amacrine and ganglion cells cause these rectifications. Thus, it can be argued (Grzywacz and Koch 1987) that they are half-wave rectifications (for both the ON and OFF inputs) and that the excitatory filter is band-pass, which requires setting $\bar{S}_e(0, 0) = 0$ in (2). It follows that the ON-OFF inputs can be defined from (1) as:

$$\begin{aligned} z_{e,\,\mathrm{on}} &= R(z_e); \qquad z_{i,\,\mathrm{on}} = z_i; \\ z_{e,\,\mathrm{off}} &= R(-z_e); \qquad z_{i,\,\mathrm{off}} = -z_i, \end{aligned} \tag{3a}$$

where R is a smooth function that satisfies $d^2R(x)/dx^2 > 0$, that is, R is supralinear in the range of interest. This form of rectification is static and we neglect saturation, since the stimulus contrast is low. For the simulations in this paper, we use

$$R(x) = A(x - T_0) + \frac{A}{2\alpha} \log(1 + e^{-2\alpha(x - T_0)}), \tag{3b}$$

where A, α, and T_0 are positive constants. (This equation comes from the integral from $-\infty$ to x of the hyperbolic tangent. The equation is positive, increases monotonically, tends to zero as x tends to $-\infty$, and approaches Ax asymptotically for x very large and positive. The two main parameters of the equation have the following meaning: T_0 is the threshold value of x for the transition between the near zero and the rising phase of the function and α is the steepness of this transition. For simulations of the rectified-quadratic model we typically set $T_0 = 0$.

Now, we introduce the quadratic nonlinearity that gives rise to directional selectivity. In general, in the lack of rectifications, this nonlinearity may be expressed as (Poggio and Reichardt 1973; Grzywacz and Koch 1987):

$$\begin{aligned} y(t) = Q(z_e, z_i) &= h_0 + h_{10} * z_e(t) + h_{01} * z_i(t) \\ &+ h_{20} *^2 z_e(t) z_e(t) + h_{11} *^2 z_e(t) z_i(t) \\ &+ h_{02} *^2 z_i(t) z_i(t), \end{aligned} \tag{4}$$

where y is the directionally-selective system's response, $*$ represents convolution, and $*^2$ is defined as:

$$\begin{aligned} h_{j_e, j_i} *^2 z_e^{j_e} z_i^{j_i} = \int_{-\infty}^{\infty} \int_{-\infty}^{\infty} dt_1\, dt_2 h_{j_e, j_i}(t_1, t_2) \\ \times \prod_{j=1}^{j_e} z_e(t - t_j) \prod_{j=1}^{j_i} z_i(t - t_{j_e + j}), \end{aligned} \tag{5}$$

where $j_e + j_i = 2$. Equation 4 is a quadratic nonlinearity, because z_e interacts at most once with itself or z_i, and vice versa. In fact, this is the most general form of quadratic nonlinearity for a two-filter interaction. This nonlinearity includes, as particular cases, multiplication (Hassenstein and Reichardt 1956; van Santen and Sperling 1984) and squaring (Adelson and Bergen 1985; Heeger 1987; Grzywacz and Yuille 1990), and generalizes for the multi-filter case (Poggio and Reichardt 1973; Grzywacz and Koch 1987).

To mix rectifications with quadratic nonlinearities, we assume that the ON and OFF inputs are independent; as supported by anatomical data (Famiglietti et al. 1977; Amthor et al. 1984, 1989). Thus, $y(t) = Q_{on}(z_{e,on}, z_{i,on}) + Q_{off}(z_{e,off}, z_{i,off})$, where Q_{on} and Q_{off} are quadratic functionals of the type defined in (4). Having to use different functionals for the ON and OFF pathways cannot be ruled out when modeling directionally selective cells. One often observes differences between the responses to light onset and light offset. In our model, these differences may arise in the interaction between the excitation and the inhibition, or in the linear preprocessing (not included in this paper).

The high-threshold mechanism for directional selectivity can be modeled as $y(t) = T(z_e(t) - z_i(t))$, where T is a function such that $T(x) = 0$ if $x \leqslant T_0$ ($T_0 > 0$), and $T(x) > 0$, $dT(x)/dx \geqslant 0$, and T is smooth if $x > T_0$. (As in (3), this form of threshold is static. Also, the mathematical statements that we give in the next section on the high-threshold model require, strictly speaking, that T is zero below threshold. This may not be the case for neural threshold mechanisms. However, computer simulations show that in practice this condition may be relaxed if the values of T after threshold are much higher than before threshold. For example, for this paper's simulations with high-threshold mechanisms, we used (3b) with $T_0 > 0$. Finally, it can be shown that inclusion of rectifications on the high threshold model does not change this paper's conclusions).

3 Predictions

This section introduces two experimental paradigms for which the three models make different predictions. The first is the measurement of the frequency content of the response waveform elicited by a drifting spatially sinusoidal grating. The second is the comparison between the average responses to drifting spatially periodic inputs and their Fourier components presented in isolation.

Let us start with a drifting spatially sinusoidal grating. In the Fourier decomposition of the directionally selective system's response, are there any harmonics higher than the second harmonic? In a purely-quadratic system, no temporal frequency of the Fourier decomposition of the output should be greater than twice that of the input (Thorson 1966; Geiger and Poggio 1975; Grzywacz and Koch 1987). On the other hand, the rectified-quadratic and the high-threshold models predict temporal frequencies that are larger than twice that of the input.

The model's temporal response to a drifting spatially sinusoidal grating is periodic, and thus have a Fourier series decomposition:

$$y(t) = y_0 + \sum_{j=1}^{\infty} y_j \cos(j\omega t + \psi_j), \qquad (6)$$

where the y_j are the Fourier coefficients (positive) and the ψ_j's the phases of the components. The following result is then general:

The response to sine-wave gratings of purely-quadratic models, that is, those models governed by (1) and (4), is such that $y_j = 0$ for $j > 2$. The same is not true for the rectified-quadratic and high-threshold models.

Now, focus on the average response to a general drifting periodic input. Decompose this input into its Fourier components, present each one of them to the directionally selective system, and record their average response. What is the larger quantity: the sum of the average responses to the components or the average response to the original input?

The three models make different predictions for the subtraction of the sum of the Fourier component responses from the original response. In a purely-quadratic system, this subtraction should be zero (Poggio and Reichardt 1973; Geiger and Poggio 1975; Grzywacz and Koch 1987). On the other hand, for a high-threshold model, this subtraction is positive (Fig. 2). Finally, in the rectified-quadratic model this subtraction may be negative (Fig. 2).

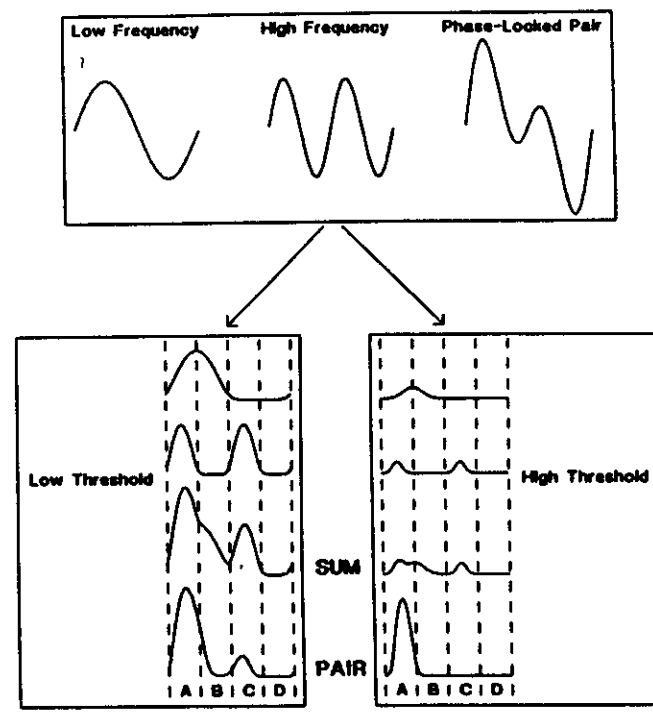

Fig. 2. Predictions for the responses of high-threshold and low-threshold (rectification) mechanisms to a periodic stimulus and to its Fourier components. The intention here is to explain the possible difference between the rectified-quadratic and high-threshold models. To do so, the full models are not needed. We simulate part of the quadratic-rectified model, namely a low-threshold mechanism, and simulate a high-threshold mechanism. Both mechanisms are simulated with (3b) ($\alpha = 3$), with low and high thresholds being $T_0 = 0$ ($A = 1$) and $T_0 = 1$ ($A = 2$) respectively. The inputs to the simulation are two sinusoidal gratings and their phase-locked pair. The responses to the sinusoids appear in the top two traces of the lower panels and that to the phase-locked pair appears in the bottom. The third trace is the sum of the top two. While the integral of this trace is larger than that of the phase-locked trace for the low threshold mechanism, the opposite holds for the high threshold mechanism. In the former case, the phase-locked trace is smaller, because for it, the negative portions of the sinusoids contribute to the calculation (Quadrants *B* and *C*). In the latter case, the individual sinusoids are almost subthreshold, but the compounded stimulus is not (Quadrant *A*)

More formally, the average response to the original stimulus $(I_0 + \gamma \sum_{j=1}^{\infty} I_j \cos(j(x/\lambda - t\omega) + \phi_j))$ is

$$\langle y \rangle = \frac{\omega}{2\pi} \int_0^{2\pi/\omega} dt\, y(t) \qquad (7)$$

Now, denote the average response of the directionally selective system to the stimulus $I_0 + \gamma I_j \cos(j(x/\lambda - t\omega))$ by $\langle y \rangle_j$. If the system's response to the stimulus I_0 is zero (as is for the cells investigated in this paper), then the following general results hold:

The purely-quadratic model predicts that $\langle y \rangle = \sum_{j=1}^{\infty} \langle y \rangle_j$.

In a high-threshold model, there exists a $\delta > 0$, *such that if* γ *satisfies* $\delta > \gamma M - T_0 > 0$, *where* $\gamma M = \max_{0 \le t < 2\pi/\omega} (z_e - z_i)$ *is defined for the stimulus presented with all its Fourier components, then* $\langle y \rangle > \sum_{j=1}^{\infty} \langle y \rangle_j$.

For the rectified-quadratic model, it is possible that $\langle y \rangle < \sum_{j=1}^{\infty} \langle y \rangle_j$.

These three conclusions are true even if $I_j = 0$ for all $j > j_0 \geq 2$.

Methods

We tested whether the predictions of the previous section apply to ON-OFF directionally selective ganglion cells of the rabbit retina. These cells have been well studied physiologically (Barlow and Levick 1965; Oyster 1968; Mistler et al. 1985), morphologically (Amthor et al. 1984, 1989), and pharmacologically (Ariel and Daw 1982), and their properties are similar to directionally selective ganglion cells in other retinas (Ariel and Adolph 1985). Extracellular responses to drifting single and phase locked pairs of low contrast sinusoidal gratings were investigated.

We recorded in an isolated eyecup preparation (Miller and Dacheux 1975; Ames and Nesbett 1981). A Tektronix 608 monitor, driven by a Picasso waveform generator (Innisfree, Cambridge, Mass), stimulated the cells. An Apple II+ computer controlled the generator. The image from the monitor covered an area that was five to ten times that of the receptive field center. The stimuli were two low contrast drifting sinusoidal gratings presented first singly and then in phase-locked pairs. Each grating or pair moved first in the preferred and then in the null direction. The spatial frequencies, whose ratio was 2:1, were chosen to elicit a near optimal response. (The low spatial frequency was about 1 cycle/deg, and the temporal contrast frequency was approximately 1 Hz). After a delay to allow the cell to reach equilibrium, the computer accumulated spike histograms over multiple cycles for each stimulus presentation, and then over multiple presentations of the series. The gratings were presented in the same order for the same period for each presentation. Both grating contrasts were close to the minimum which elicited statistically significant directional selectivity (1% to 5%).

We recorded the responses from forty directionally selective cells in twenty three retinas. The analysis here is based on five cells that met our criterion of statistically significant directionally selective responses below a stimulus contrast of 5%. This criterion is critical, because our models only hold for low contrast. At high contrasts, our approximations are no longer valid and nonlinearities unrelated to directional selectivity may "contaminate" the data. Thus, to be in the models' validity range, we investigated a small sample of cells, which nevertheless, included the cells that were the most sensitive for direction of motion.

Results

We divide this section in two parts as follows. The first, "Second Harmonic", describes the second harmonic content among high harmonics in the cells' responses to a drifting spatially sinusoidal grating. The second, "Superposition", reports the difference between the cells' average response to a superposition of two drifting sinusoidal gratings and the sum of their average responses when presented in isolation. In both parts, model predictions and results are compared.

1 Second harmonic

In this section, we report the frequency-content analysis of the response waveform elicited by drifting spatially sinusoidal inputs whose contrasts were close to the minimum required to elicit directionally selective responses. Figure 3 shows the mean poststimulus histogram of a directionally selective cell and the histogram's Fourier spectrum for motion in the preferred direction.

The energies in the second, third, and fourth harmonics are significantly above zero. This significance is demonstrated by a statistical analysis of the run-to-run values of the complex Fourier components at each frequency. We consider a harmonic to have significant energy, if either its real or its imaginary part is different than zero with a probability larger than 0.99 (two-sided t test).

Figure 4 plots, for the other four cells, the Fourier spectra of their mean poststimulus histogram for motion in the preferred direction. Once again, these spectra contain significant energies in harmonics higher than the second. The only cell without significant high harmonics is cell E358.c1.

The purely-quadratic model is inconsistent with this result. As we discussed after (6), this model predicts that the highest possible harmonic in the response is the second. However, that cell E358.c1 has only statistically significant first and second harmonics does not mean that a purely-quadratic model mediates this cell's directional selectivity. In the section "Superposition", it is shown that another experiment rules out this model for this cell. Thus probably, this cell had harmonics higher than second in its response, but they were buried under the noise.

In summary, the cells' temporal responses to drifting spatially sinusoidal gratings of low contrast are consistent with rectified-quadratic and high-threshold models, but not with a purely-quadratic model.

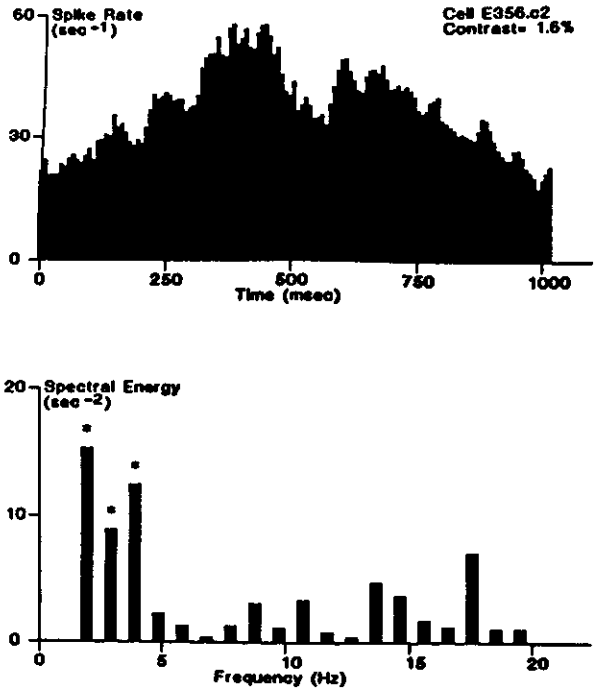

Fig. 3. Mean poststimulus histogram and its Fourier spectrum. *Top* The mean poststimulus histogram of a directionally selective cell's response to a sinusoidal grating drifting in the preferred direction. A cycle of sinusoidal grating determined the total duration of the histogram. The histogram is filtered by a five bin moving-average window, which corresponds to a filter whose 3 dB frequency is at 10.8 Hz. The dip just after 500 ms is real with the corresponding maxima being characteristic of the cell's ON-OFF responses. *Bottom* The spectral energies of the unfiltered poststimulus histogram. Here, the spectral energy at a given frequency is defined as the sum of the squares of the Fourier coefficients at that frequency. Only the frequencies up to the twentieth harmonic are shown and the units of the horizontal axis are multiples of the fundamental frequency. The energy at the fundamental frequency is not shown, since it is much higher than the vertical axis. The stars mark the harmonics that are statistically significant on a run-to-run test of the complex Fourier components at each frequency (see text for a description of the test). Not consistently with the purely-quadratic model, the third and fourth harmonics are significant. However, this result is consistent with the rectified-quadratic and high-threshold models

2 Superposition

Now, we show the results of the comparison between the average responses to drifting spatially periodic inputs and their Fourier components presented in isolation. Here, we used two low contrast sinusoidal gratings drifting in isolation or in phase locked pairs. The grating's spatial frequencies were in a 2:1 ratio. (In the phase-locked case, two phase differences were used with similar results. In the first, the extrema of the low-spatial frequency grating coincided with the gradient minima of the high-spatial frequency grating. In the second, the coincidence was with the gradient maxima. Since the results were similar for both phases, we report only their pooled results.) The gratings and grating pairs were each presented for an integer number of the low-frequency cycles, and this sequence was repeated for a large number of trials. Following the definitions after (7), we denote the average spike rate in the prefered direction of the low frequency, high frequency, and the phase locked gratings, by $\langle y\rangle_1$, $\langle y\rangle_2$, and $\langle y\rangle$ respectively. The distribution of the values of $\langle y\rangle - \langle y\rangle_1 - \langle y\rangle_2$ over seventy trials for one cell is shown in Fig. 5.

The sum of the average responses to the isolated components is larger than their phase locked average. In other words, the distribution is biased towards negative values, which means that $\langle y\rangle < \langle y\rangle_1 + \langle y\rangle_2$. This negative bias is statistically significant on a nonparametric rank-signed Wilcoxon test ($p < 0.0001$).

To quantify this lack of superposition, we use the *index of superposition of nonlinearities* of Grzywacz and Koch (1987). This index is

$$y_{sn} = \frac{\langle y\rangle - (\langle y\rangle_1 + \langle y\rangle_2)}{\langle y\rangle + (\langle y\rangle_1 + \langle y\rangle_2)}. \tag{8}$$

The reason for why this index quantifies the lack of superposition is as follows. The more the superposition holds, the closer y_{sn} is to 0, and the less it holds, the closer $|y_{sn}|$ is to 1. If $\langle y\rangle > \langle y\rangle_1 + \langle y\rangle_2$, then $y_{sn} > 0$, and if $\langle y\rangle < \langle y\rangle_1 + \langle y\rangle_2$, then $y_{sn} < 0$. (The name "index of superposition of nonlinearities" was given, because even for purely-quadratic models where this index is zero, there is no superposition in the linear sense. This index measures *superposition in the average* for nonlinear systems. For a discussion of the superposition-in-the-average property see Poggio and Reichardt 1973, Geiger and Poggio 1975.)

Figure 6 displays the index of superposition of nonlinearities for all five cells and shows that the index is negative, which confirms the negative bias of Fig. 5.

The data of Figs. 5 and 6 are consistent with a rectified-quadratic model but not with purely-quadratic or high-threshold models. The conclusions after (7) say that superposition should hold for a purely quadratic model. This implies a prediction of no bias for Fig. 5 and a zero index of superposition of nonlinearities. Also, after (7) and in Fig. 2, we saw that the high-threshold model predicts positive values for the bias and the index. On the other hand, the rectified-quadratic model may give rise, correctly, to negative values.

One might object that the present experiments only probed the behavior of cells at low contrasts (<5%), and maybe missed purely-quadratic behavior at higher contrasts. In part to avoid such objections, we measured informally the responses of several cells to higher contrasts (<50%). These responses also could not be approximated well by a purely-quadratic model (under the tests of Fig. 3–6). From a theoretical point of view, this is not surprising. Grzywacz and Koch (1987) found that purely-quadratic models provide poor approximations to the high-contrast behavior of proposed biophysical models of retinal directional selectivity. For example, they showed that shunting-inhibition models

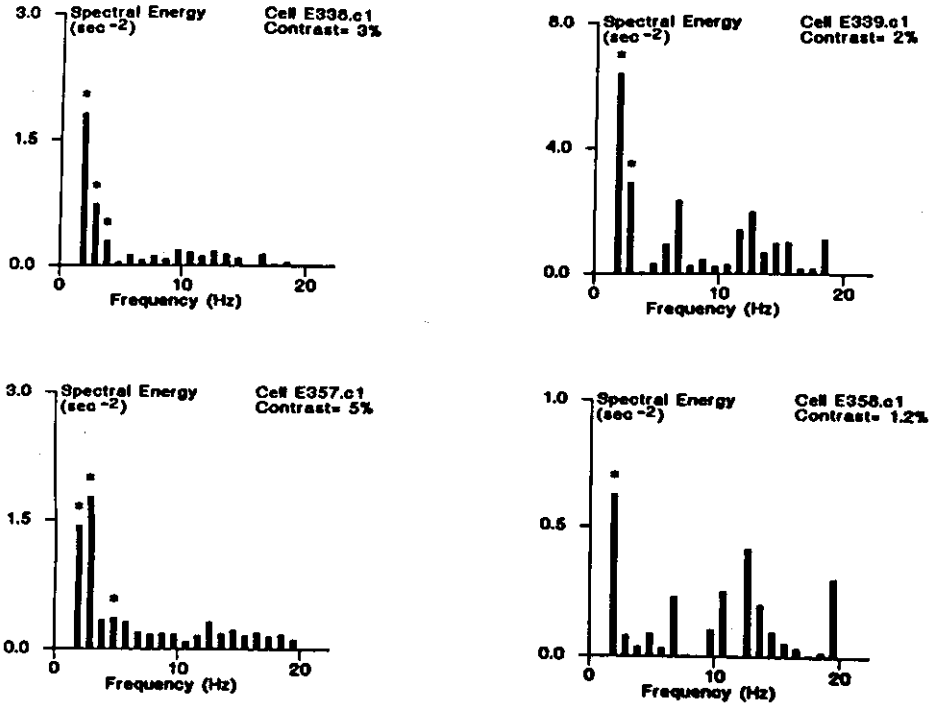

Fig. 4. Fourier spectra of the responses to sinusoidal gratings. A similar calculation like the one in Fig. 3 is performed for four more cells. As in Fig. 3, the stars mark the harmonics that are statistically significant. In three of these cells, there are harmonics significantly higher than the second, which is inconsistent with the purely-quadratic model. However, in cell E358.c1, no harmonics higher than the second are significantly above chance. The test of Figs. 5 and 6 show that the responses of this cell are, nevertheless, inconsistent with a purely-quadratic model

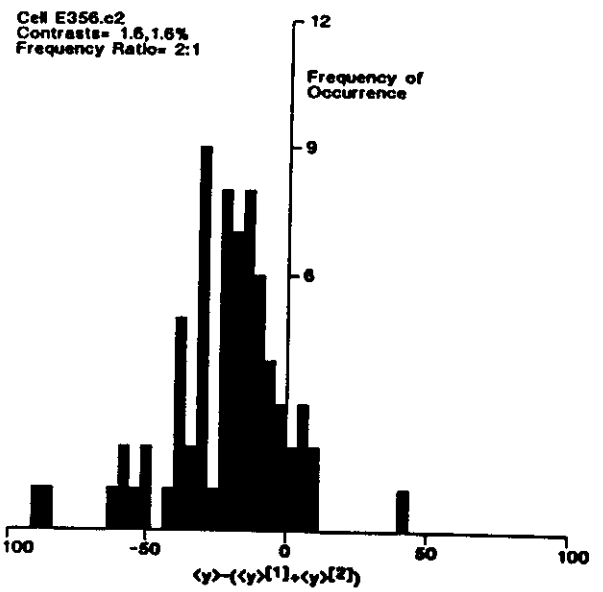

Fig. 5. Lack of average response superposition. This figure shows the histogram of the differences between the integrated response to the superimposed pair of sinusoidal gratings ($\langle y \rangle$) and the sum of the integrated responses to the same two sinusiodal gratings presented separately ($\langle y \rangle_1 + \langle y \rangle_2$). Each response was integrated over five cycles of the low-spatial frequency grating (after a delay of two cycles to allow the transient response components to decay). The histogram is skewed towards negative values. Thus, the total response to the compound grating tended to be smaller than the sum of the total responses to the isolated gratings. This inequality is inconsistent with the purely-quadratic and high-threshold models

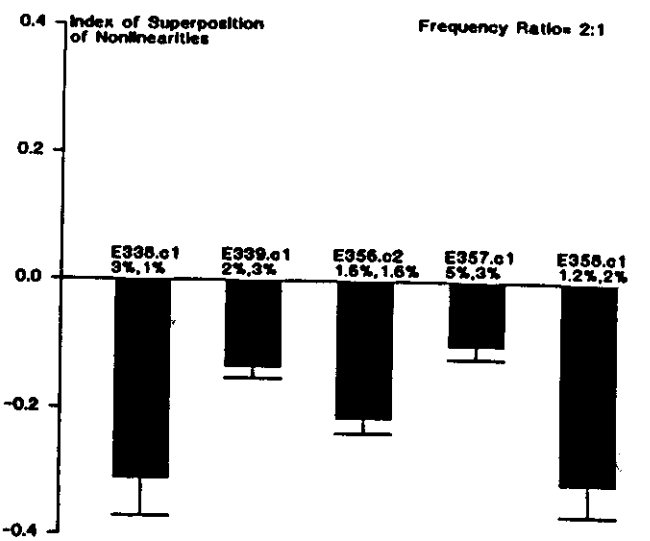

Fig. 6. The index of superposition of nonlinearities. For five cells, the mean and standard error of the index of superposition of nonlinearities (8) was calculated from distributions like the one in Fig. 5. In each bin, the first and second labeled percentages correspond to the contrasts of the low- and high-spatial frequency gratings respectively. Confirming the trend observed in that figure, the indices are significantly negative. Once again, this result is inconsistent with the purely-quadratic and high-threshold models but consistent with the rectified-quadratic model

deviate significantly from quadratic behavior for conductance modulations higher than 30%. (Shunting-conductance modulations smaller than 30% are typically not sufficient to produce strong directional selectivity – Grzywacz and Koch 1987.) In this paper, we focused on low contrast stimuli, because they were the most likely to elicit quadratic behavior.

Discussion

In conclusion, we have ruled out the class of purely-quadratic computational models (Hassenstein and Reichardt 1956; van Santen and Sperling 1984; Adelson and Bergen 1985) for the ON-OFF directionally selective cells of the rabbit. This class of models includes the correlation schemes (Hassenstein and Reichardt 1956; van Santen and Sperling 1984), which have motivated a considerable amount of research. The results are consistent with the suggestion that quadratic behavior may be rare among motion sensitive cells in the early stages of the visual pathway (Grzywacz and Koch 1987). This computationally advantageous behavior (Poggio and Reichardt 1973), if exhibited at the level of the organism, is probably due to late integrating neurons. Averaging intrinsic to such neurons, together with biological noise, could partially "linearize" the responses reducing their high order nonlinearities, and thus emphasizing their quadratic behavior (Poggio 1975). Examples of motion sensitive neurons that might work quadratically, include the complex cells of cat striate cortex (Emerson et al. 1987) and the horizontal cells in the third visual ganglion of flies (Egelhaaf et al. 1989).

The responses of ON-OFF directionally selective cells of the rabbit retina cannot also be accounted for by models based on a high threshold. The failure of such models is significant, since thresholds have perhaps been the most commonly proposed mechanism for information processing in the nervous system (Sherrington 1933). Also, they underlie several of the parallel distributed processing (PDP) models proposed so far (Rosenblatt 1962; Hopfield 1984; Rummelhart et al. 1986).

The only model considered here that is consistent with the data is the rectified-quadratic model. In this model, a quadratic interaction between linear preprocessing filters is either preceded or followed by a rectification. The quadratic interaction could be due to shunting inhibition (Thorson 1966; Torre and Poggio 1978), for which there is recent evidence in rabbit (Amthor and Grzywacz 1990). Alternatively, the quadratic behavior could arise from a linear summation followed by a low level threshold (Grzywacz and Koch 1987). The rectification, which "spoils" the quadratic behavior, may arise in the ON and OFF pathways (presynaptic to the ganglion cell), or in the spiking mechanism of the ganglion cell. (Interestingly, one can extend the superposition-of-nonlinearities test to gratings drifting with different velocities. Foxman and Victor (1987) used such an extension to study human visual evoked potentials, also finding evidence for the contribution of rectification to the responses.)

The implications of directionally selective ganglion cells using a computational strategy departing from the theoretically "optimal" purely-quadratic mechanism (Poggio and Reichardt 1973) are unclear. An explanation for this departure might simply be that the biophysics of neurons are better suited to perform other computations. This explanation agrees with the idea (Poggio 1983; Grzywacz and Poggio 1990) that the properties and limitations of neurons influence the choice of biological visual algorithms. Possibly, one such limitation is that purely quadratic nonlinearities are hard to implement neurally (Grzywacz and Koch 1987). On the other hand, rather than being a limiting factor, rectifications could be advantageous. For example, their participation in the segregation between ON and OFF pathways may increase the contrast sensitivity of the visual system (Schiller et al. 1986).

Acknowledgements. We thank Lyle Borg-Graham and Tomaso Poggio for useful comments on the manuscript. N.M.G. was supported by the grant BNS-8809528 from the National Science Foundation, by the Sloan Foundation, by a grant to Tomaso Poggio, Ellen Hildreth, and Peter Schiller from the Office of Naval Research, Cognitive and Neural Systems Division, and by the grant IRI-8719394 to Tomaso Poggio, Ellen Hildreth, and Edward Adelson from the National Science Foundation. F.R.A. was supported by grants from the National Eye Institute (EY05070) and the Sloan Foundation.

References

Adelson EH, Bergen JR (1985) Spatio-temporal energy models for the perception of motion. J Opt Soc Am A 2:284–299

Ames A, Nesbett FB (1981) In vitro retina as an experimental model of the central nervous system. J Neurochem 37:867–877

Amthor FR, Grzywacz NM (1990) The nonlinearity of the inhibition underlying retinal directional selectivity. Vis Neurosci

Amthor FR, Oyster CW, Takahashi ES (1984) Morphology of on-off direction-selective ganglion cells in the rabbit retina. Brain Res 298:187–190

Amthor FR, Takahashi ES, Oyster CW (1989) Morphologies of rabbit retinal ganglion cells with complex receptive fields. J Comp Neurol 280:97–121

Ariel M, Adolph AR (1985) Neurotransmitter inputs to directionally sensitive turtle retinal ganglion cells. J Neurophysiol 54:1123–1143

Ariel M, Daw NW (1982) Pharmacological analysis of directionally sensitive rabbit retinal ganglion cells. J Physiol 324:161–185

Barlow HB, Levick WR (1965) The mechanism of directionally selective units in rabbit's retina. J Phyiol 178:477–504

Dowling JE (1979) Information processing by local circuits: The vertebrate retina as a model system. In: Schmitt FO, Worden FG (eds) The neurosciences, fourth study program, MIT Press, Cambridge, Mass, pp 163–181

Egelhaaf M, Borst A, Reichardt W (1989) The nonlinear mechanism of direction selectivity in the fly motion detection system. Naturwissenschaften 76:32–35

Emerson RC, Citron MC, Vaughn WJ, Klein SA (1987) Nonlinear directionally sensitive subunits in complex cells of cat striate cortex. J Neurophysiol 58:33–65

Famiglietti EV, Kaneko A, Tachibana M (1977) Neuronal architecture of ON and OFF pathways to ganglion cells in carp retina. Science 198:1267–1268

Foxman B, Victor J (1987) A VEP study of flickering and moving gratings. Invest Ophthalmol Vis Sci 28:297

Geiger G, Poggio T (1975) The orientation of flies towards visual patterns: on search for the underlying functional interactions. Biol Cybern 19: 39–54.

Grzywacz NM, Koch C (1987) Functional properties of models for direction selectivity in the retina. Synapse 1:417–434

Grzywacz NM, Poggio T (1990) Computation of motion by real neurons. In: Zornetzer SF, Davis JL, Lau C (eds) An introduction to neural and electronic networks. Academic Press, New York, pp 379–403

Grzywacz NM, Yuille AL (1990) A model for the estimate of local image velocity by cells in the visual cortex. Proc R Soc London B 239:129–161

Hassenstein B, Reichardt WE (1956) Systemtheoretische Analyse der Zeit-, Reihenfolgen- und Vorzeichenauswer-tung bei der Bewegunsperzeption des Rüsselkafers *Chlorophanus*. Z Naturforsch 11b:513–524

Hausen K (1981) Monocular and binocular computation of motion in the Lobula Plate of the fly. Verh Dtsch Zool Ges 74:49–70

Heeger DJ (1987) A model for the extraction of image flow. J Opt Soc Am A 4:1455–1471

Hopfield JJ (1984) Neurons with graded response have collective computational properties like those of two-state neurons. Proc Natl Acad Sci USA 81:3088–3092

Hubel DH, Wiesel TN (1959) Receptive fields of single neurons in the cat's striate cortex. J Physiol 148:574–591

Kuffler SW (1953) Discharge patterns and functional organization of mammalian retina. J Neurophysiol 16:37–68

Marchiafava PL (1979) The responses of retinal ganglion cells to stationary and moving visual stimuli. Vision Res 19:1203–1211

Masland RH, Mills W, Cassidy C (1984) The functions of acetylcholine in the rabbit retina. Proc R Soc London B 223:121–139

Maturana HR, Lettvin JY, McCulloch WS, Pitts WH (1960) Anatomy and physiology of vision in the frog *(Rana Pipiens)*. J Gen Physiol 43 [Suppl. 2]:129–171

Miller RF, Bloomfield SA (1983) Electroanatomy of an unique amacrine cell in the rabbit retina. Proc Natl Acad Sci USA 80:3069–3073

Miller RF, Dacheux RF (1975) Chloride sensitive receptive field mechanisms in the isolated retina-eyecup of the rabbit. Brain Res 90:329–334

Mistler LA, Amthor FR, Koch C (1985) Modeling HRP-injected, physiologically-characterized direction-selective ganglion cells in rabbit retina. Invest Ophthalmol Vis Sci 26:165

Oyster CW (1968) The analysis of image motion by the rabbit retina. J Physiol 199:613–635

Poggio T (1975) Stochastic linearization, central limit theorem and linearity in (nervous) 'black-boxes'. Atti del III Congresso di Cibernetica e Biofisica, pp 349–358

Poggio T (1983) Visual algorithms. In: Braddick OJ, Sleigh AC (eds) Physical and biological processing of images, Springer, Berlin Heidelberg New York, pp 128–153

Poggio T, Reichardt WE (1973) Considerations on models of movement detection. Kykbernetik 13:223–227

Rosenblatt F (1962) Principles of neurodynamics. Spartan, New York

Rummelhart DE, Hinton GE, Williams RJ (1986) Learning representations by back-propagating errors. Nature 323:533–536

Schiller PH, Finlay BL, Volman SF (1976) Quantitative studies of single-cell properties in monkey striate cortex. I. Spatiotemporal organization of receptive fields. J Neurophysiol 49:1288–1319

Sherrington CS (1933) The brain and its mechanism. Cambridge University Press, London

Thorson J (1966) Small-signal analysis of a visual reflex in the locust. II. Frequency dependence. Kybernetik 3:52–66

Torre V, Poggio T (1978) A synaptic mechanism possibly underlying directional selectivity to motion. Proc R Soc London Ser B 202:409–416

Schiller PH, Sandell JH, Maunsell JHR (1986) Function of the ON and OFF channels of the visual system. Nature 322:824–825

Van Santen JPH, Sperling G (1984) A temporal covariance model of motion perception. J Opt Soc Am A 1:451–473

Victor JD, Shapley RM (1979) The nonlinear pathway of Y ganglion cells in the cat retina. J Gen Physiol 74:671–689

Watanabe S-I, Murakami M (1984) Synaptic mechanisms of directional selectivity in ganglion cells of frog retina as revealed by intracellular recordings. Jpn J Physiol 34:497–511

Dr. Norberto M. Grzywacz
The Smith-Kettlewell Eye Research Institute
2232 Webster Street
San Francisco, CA 94115
USA